

Alma Mater Studiorum Università di Bologna
Archivio istituzionale della ricerca

Torque Penetrometric Test for the in-situ characterisation of historical mortars: fracture mechanics interpretation and experimental validation

This is the final peer-reviewed author's accepted manuscript (postprint) of the following publication:

Published Version:

Marastoni, D., Benedetti, A., Pelà, L., Pignagnoli, G. (2017). Torque Penetrometric Test for the in-situ characterisation of historical mortars: fracture mechanics interpretation and experimental validation. CONSTRUCTION AND BUILDING MATERIALS, 157, 509-520 [10.1016/j.conbuildmat.2017.09.120].

Availability:

This version is available at: <https://hdl.handle.net/11585/621391> since: 2018-02-12

Published:

DOI: <http://doi.org/10.1016/j.conbuildmat.2017.09.120>

Terms of use:

Some rights reserved. The terms and conditions for the reuse of this version of the manuscript are specified in the publishing policy. For all terms of use and more information see the publisher's website.

This item was downloaded from IRIS Università di Bologna (<https://cris.unibo.it/>).
When citing, please refer to the published version.

(Article begins on next page)

This is the final peer-reviewed accepted manuscript of:

*Diego Marastoni, Andrea Benedetti, Luca Pelà, Giacomo Pignagnoli, **Torque Penetrometric Test for the in-situ characterisation of historical mortars: fracture mechanics interpretation and experimental validation**, Construction and Building Materials, Volume 157, 2017, Pages 509-520, ISSN 0950-0618*

The final published version is available online at:

<https://doi.org/10.1016/j.conbuildmat.2017.09.120>

Rights / License:

The terms and conditions for the reuse of this version of the manuscript are specified in the publishing policy. For all terms of use and more information see the publisher's website.

This item was downloaded from IRIS Università di Bologna (<https://cris.unibo.it/>)

When citing, please refer to the published version.

Torque Penetrometric Test for the In-Situ Characterisation of Historical Mortars: Fracture Mechanics interpretation and experimental validation

Diego Marastoni ^a, Andrea Benedetti ^a, Luca Pelà ^{b*}, Giacomo Pignagnoli ^a

a) Department of Civil, Chemical, Environmental and Materials Engineering, University of Bologna, Viale Risorgimento 2, 40136 Bologna, Italy.

b) Department of Civil and Environmental Engineering, Universitat Politècnica de Catalunya (UPC-BarcelonaTech), Jordi Girona 1-3, 08034 Barcelona, Spain

* Corresponding author. Email: luca.pela@upc.edu

Abstract – The assessment of historical structures requires appropriate knowledge of the behaviour of the investigated materials. Concerning masonry, its mechanical characterisation is a challenging task, since its composite nature requires the careful evaluation of the behaviour of its material components. In particular, the experimental assessment of the strength of existing mortar in historical structures still encounters several difficulties. This study investigates a novel Minor Destructive Testing technique virtually equivalent to the vane test used for soil investigation. The instrumentation, called herein Torque Penetrometric Test, is composed of a steel nail with four protruding teeth and a torque wrench. The test consists in inserting the toothed nail into a mortar joint and then applying a torque to it by means of a dynamometric key until reaching the failure of the material. This work presents a novel interpretation theory based on basic fracture mechanics concepts applied to the micro-mechanical analysis of the stress state induced by the instrument on the investigated mortar. The proposed interpretative theory is validated through the execution of experimental tests in the laboratory and on an existing historical masonry building. The test proves to be effective for a quick in-situ MDT evaluation of the strength of existing mortars.

24 *Keywords: Historical Construction; Masonry; Brickwork; Mortar; In-situ Testing; Minor Destructive Testing*
25 *(MDT); Compressive Strength; Penetrometric Test; Fracture Mechanics; Fracture Energy.*

26 Abbreviations - MDT: Minor Destructive Testing;
27 NDT: Non Destructive Testing;
28 TPT: Torque Penetrometric Test;
29 DPT: Double Punch Test;
30 DFJ: Double Flat Jack.

32 **Highlights**

- 33 • Novel torque penetrometer for the in-situ mechanical characterization of mortar
- 34 • Toothed nail inserted into the mortar and twisted with a torque-meter until failure
- 35 • Proposal of test interpretation theory based on fracture mechanics
- 36 • Interpretation theory validated using new and available experimental campaigns
- 37 • In-situ applications prove the reliability of the instrument for historical mortars

39 **1. Introduction**

40 The structural assessment of historical buildings has become a fundamental topic in the conservation of the
41 built cultural heritage, especially in the last decades where significant catastrophic events have threatened many
42 important constructions [1,2]. Concerning monuments, the evaluation of the structural health and the
43 identification of possible vulnerabilities can allow the minimization of strengthening work and thus the
44 preservation of their original cultural value.

45 The conservation and protection of historical structures require a multidisciplinary approach involving a variety
46 of professional skills. For this reason, the ICOMOS in 2003 produced a recommendation list [3] in order to

47 assist and advice the professionals involved in the assessment of historical masonry buildings. The proposed
48 approach is defined as “Knowledge-Based Assessment” and requires information about the original structural
49 conception, the construction techniques, the existing damage and the modifications occurred in the building’s
50 life. Both qualitative and quantitative approaches can be adopted in the diagnosis. Notwithstanding the
51 importance of the qualitative approach based in a direct recognition of the monument, the quantitative approach
52 is fundamental in establishing the mechanical data necessary for the analysis phase. In this context, it is
53 convenient to organise different levels of experimental activities, starting with the simpler and less invasive
54 ones, to be complemented with more sophisticated and destructive only in few selected positions.

55 The experimental characterisation of masonry requires the evaluation of the properties of the constituent
56 materials, i.e. units (stone or brick) and mortar (cement, lime, etc.). With the development of new technologies
57 in the experimental testing of masonry constructions, several NDT techniques were proposed to obtain
58 information on the structure without damaging it. Most of NDT methods are based on the transmission of sonic
59 or electromagnetic waves through the material. The sonic test [4] has shown its suitability in the estimation of
60 the elastic properties of the materials, also allowing the determination of internal defects or discontinuities. The
61 Ground Penetrating Radar (GPR) can detect the presence of voids, structural irregularities, different materials
62 or moisture inside the existing masonry. The complementary use of these investigation techniques is a common
63 practice in order to improve the reliability of the NDT results.

64 Several standards and recommendations for the assessment of historical structures [5] suggest to combine NDT
65 and laboratory testing to improve the level of knowledge of the materials’ properties. This approach is usually
66 considered in works dealing with the assessment of historical masonry buildings [6].

67 Fully destructive tests are not possible in historical structures since all the experimental activities must respect
68 their intrinsic heritage value. For this reason, recent research is addressing the development of efficient Minor
69 Destructive Testing (MDT), based either on penetrometric techniques or extraction of small samples of
70 masonry to be tested in the laboratory [7–12].

71 Penetrometric techniques are classified in the literature either as MDT or NDT [7], since the entity of damage
72 induced to the structure is minimal. These tests are performed directly on the material to investigate, requiring

73 the removal of plaster or coating surfaces. The penetrometric tests for masonry are usually modified versions of
74 micro-destructive techniques available for other materials (mainly concrete).

75 The Pin Penetration Test, also known as Windsor Probe, was initially designed for hardened concrete
76 investigation according to the US standards [13]. The system uses a metal pin driven into the material since the
77 recorded depth of penetration can be easily correlated to the material's compressive strength. Recent works
78 about the application of such technique to low-strength mortars can be found in [12,14].

79 Schmidt Hammer test is also well-known as NDT for concrete [15]. In this the compressive strength case is
80 correlated to the material's superficial hardness. Using this principle, Van Der Klugt [16] proposed a pendulum
81 hammer for the quality assessment of the masonry joints.

82 DRMS (Drilling Resistance Measurement System) method investigates the mortar strength [17] by measuring
83 the force necessary to penetrate a compact material. Other researchers have developed different types of
84 penetrometers [18,19], using the basic principles of the Standard Penetration Test (SPT) used in soil
85 characterisation.

86 Recently, Christiansen proposed a torque penetrometer called X-Drill [20] consisting of a four-teeth nail made
87 of stainless steel. A 6 mm diameter pilot hole is executed in order to drive the instrument into the mortar joint.
88 The test is carried out by using a torque-meter that measures the maximum torque M_v resisted by the material.
89 The author presented experimental relationships between the laboratory compressive strengths of some types of
90 mortars and the corresponding values of torque obtained with the X-Drill.

91 This paper presents a MDT penetrometric technique called Torque Penetrometric Tests (TPT). This apparatus
92 for in-situ testing is based on the procedures of both the geotechnical vane test and the X-Drill technique, but it
93 provides important conceptual improvements in order to obtain more reliable experimental results [21]. This
94 study presents a new mechanical interpretation theory of the TPT based on a fracture energy equilibrated
95 model. The proposed approach provides a simple analytical expression for the evaluation of the compressive
96 strength of existing mortars. All the parameters of the proposed model are calibrated by means of experimental
97 data available in the existing literature for several types of mortar.

98 The TPT technique and its interpretation theory were calibrated by considering a representative set of mortar
99 specimens built in the laboratory with different compositions, corresponding to a rather wide range of
100 compressive strengths. The comparison between the TPT measurements and the standard laboratory
101 compression tests on the set of specimens provided the basic results for the interpretation of the TPT response
102 [21]. Additional calibration data were gathered from experiments available in the literature [20]. Finally, the
103 paper presents the results of real applications on a masonry wall built in the laboratory with historical-like
104 materials [9,10], as well as on the existing masonry walls of an historical building struck by the 2012 Emilia-
105 Romagna earthquake.

106

107 **2. Description of the apparatus**

108 The apparatus proposed in this research for MDT of historical mortars is called from now on as Torque
109 Penetrometric Tests (TPT) [21]. It is composed of a nail with four teeth and a torque wrench. The nail is
110 obtained by shaping a class 8.8 steel screw (characteristic tensile and yield strengths: 800 MPa and 640 MPa)
111 with a lathe, and then manufacturing the teeth with a mill (Figure 1). This material was chosen for its high
112 performance, reducing the risk of torque failure of the nail during the test. The cost of the device is limited due
113 to both the large availability of the material and the easy manufacturing.

114



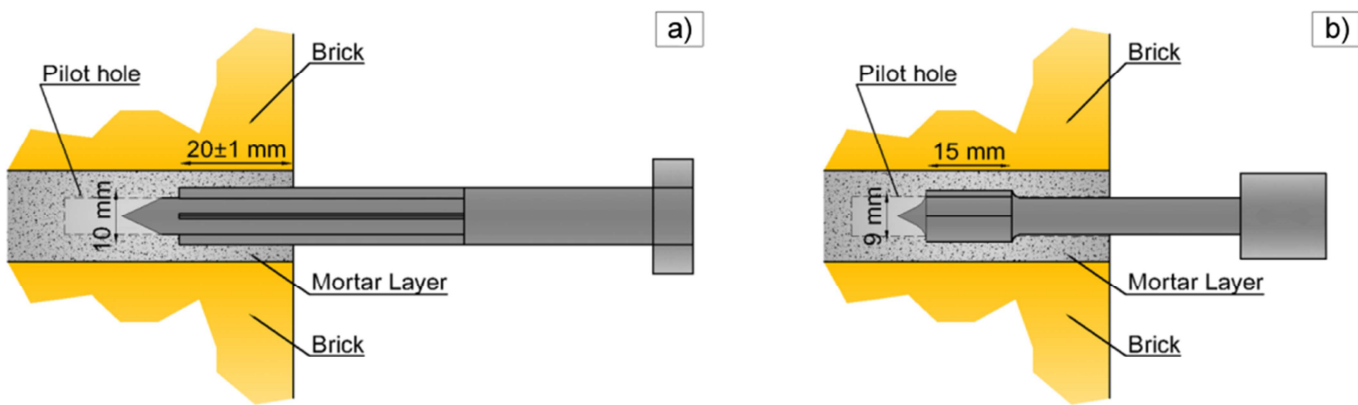
115

116 Figure 1 - Novel nail proposed for the Torque Penetrometric Test of historical mortars [21].

117

118 The geometry of the novel instrument was studied in order to reduce the sources of uncertainties of the testing
 119 technique, as well as the drawbacks detected in previous studies. Christiansen's X-Drill [20] was characterised
 120 by a fully toothed shank with an external diameter of 10 mm and an internal diameter of 6.5 mm. The X-Drill
 121 methodology required the measurement of the depth of investigation L_w at each test, set in the range between 15
 122 mm and 20 mm [20]. This operation introduced L_w as a further uncertainty in the problem (see Figure 2a), since
 123 the errors related to the estimation of the variable L_w affected also the evaluation of the ultimate normalised
 124 torque $m_v = M_v / L_w$ to be related with the material's compressive strength. Furthermore, the fully toothed shank of
 125 the X-Drill allowed the investigation of the sole external part of the mortar joint (see Figure 2a) which, in case
 126 of existing masonry, could be either deteriorated by environmental actions or composed of newly repointed
 127 material. This problem may lead to rather superficial measurements and thus to possible erroneous estimations
 128 of the mechanical properties of mortar. Finally, the outer diameter of the cross section of the X-Drill was 10
 129 mm. This dimension results comparable with the thickness of the mortar joints in existing brickwork. In fact,
 130 when the existing mortar joints are about 10 mm thick, the X-Drill might hit the bricks' surfaces during the test,
 131 yielding results biased by the contacts with a different and more resistant material.

132



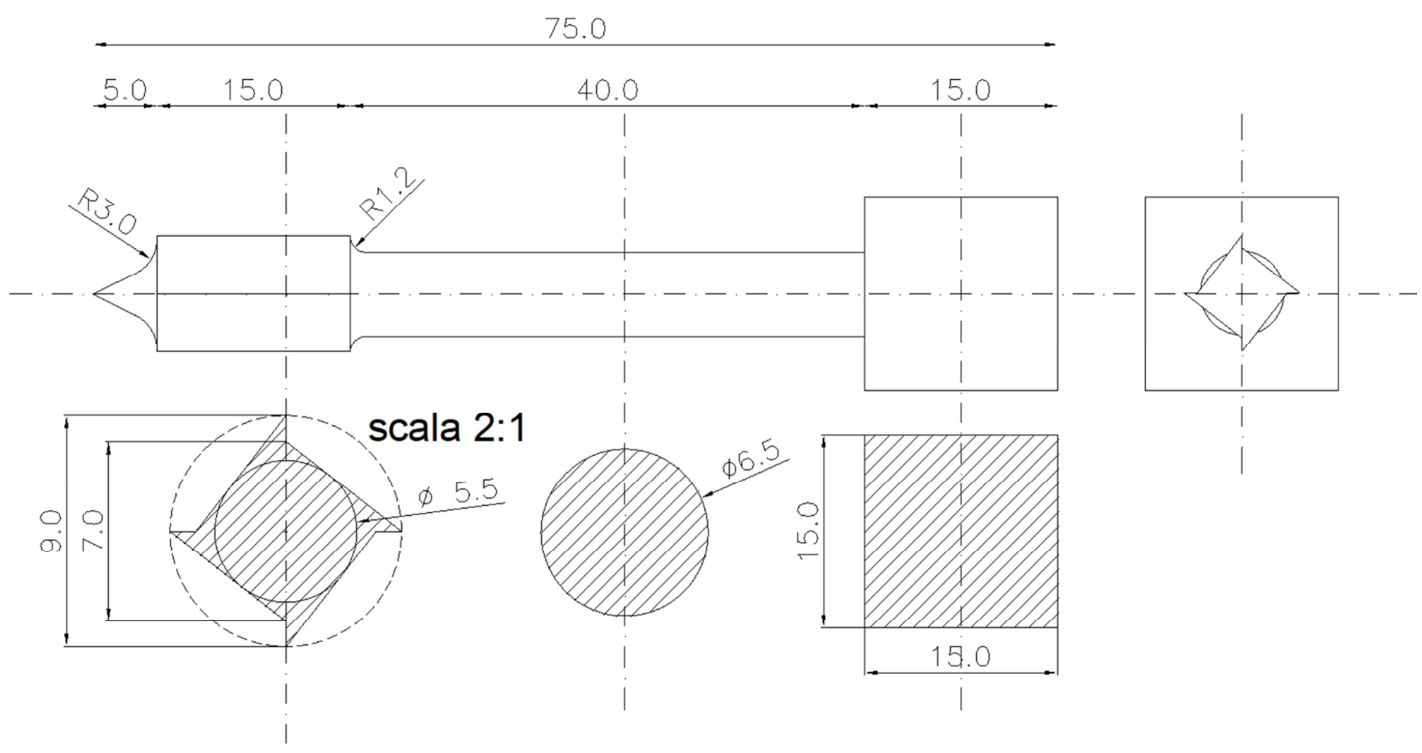
133

134 Figure 2 - Longitudinal section of the X-Drill [20] (a) and the novel TPT proposed in this work (b)

135

136 On the other hand, the proposed TPT presents important technical improvements in order to overcome the
 137 aforementioned limitations, as shown in Figure 2 and Figure 3. First, the toothed part of the nail's shank is only
 138 15 mm long in order to remove the aleatory error related to the measurement of L_w parameter. The remaining

139 part of the nail's shank has a smooth cylindrical shape with 6.5 mm diameter. This solution grants a constant
 140 depth of investigation $L_w = 15$ mm. In fact, once the instrument is completely inserted into the material, only
 141 the nail's teeth can be effectively in contact with mortar, whereas the remaining length of the shank cannot (see
 142 Figure 2b). Second, the TPT apparatus developed in this research allows a deeper insertion of the toothed nail,
 143 testing an inner volume of material and bypassing the external layer of the mortar joint (see Figure 2b). The
 144 shaft length of 40 mm assumed in this research (see Figure 3) could be modified on the basis of the
 145 experimental needs. Finally, the external diameter of the novel toothed nail is reduced to 9 mm (Figure 2b)
 146 trying to avoid experimental results spoiled by the undesired contact with the bricks.
 147

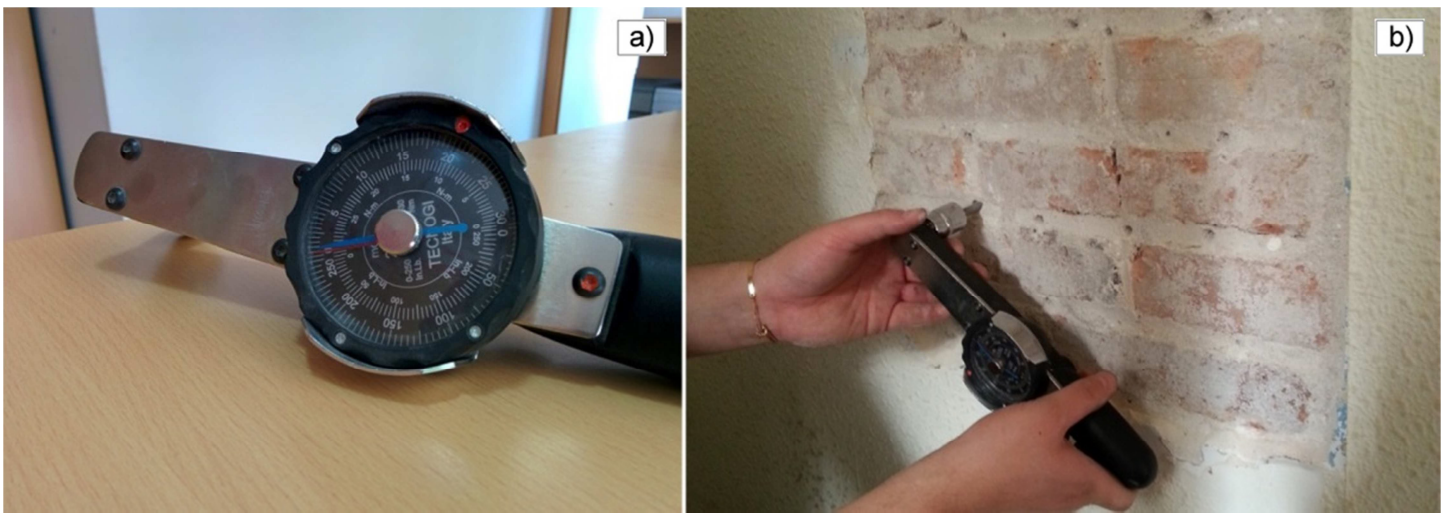


148
 149 Figure 3 – Technical drawings with specifications and dimensions of the TPT used in this research.

150
 151 Precise working operations of the TPT are proposed to provide a robust procedure against possible execution
 152 mistakes. The first step is the realization of a 7 mm diameter pilot hole to drive the instrument into the mortar
 153 joint. Whilst drilling the mortar to execute the pilot hole, the user must check that no brick powder is extracted
 154 and that the rate of advance is regular and constant. These two checks are necessary to exclude the presence of

155 bricks or cavities along the track of the pilot hole. The second step is the hammering of the TPT shaft inside the
156 pilot hole. The specific geometry of the system (see Figure 3) allows the toothed part to be inserted into the
157 pilot hole while avoiding directional deviations from the hole axis. The third step consists in the use of a torque
158 wrench to measure the torque necessary to bring the material to failure. This research considered a
159 dynamometric torque wrench equipped with an analogic display with $0 \div 30 \text{ Nm}$ range and $\pm 0.5 \text{ Nm}$ precision.
160 Figure 4 shows the torque wrench used for the execution of the tests. The readings could be done using either
161 analogic or digital torque wrenches. These two different typologies can have almost the same measurement
162 range, but in general the resolution of the digital transducer is higher than the analogic one, although the
163 precision can be very similar since it is based on the quality of the device. The last step of the TPT operation is
164 the removal of the toothed nail from the mortar joint. A final visual check is necessary to control the material
165 in-between the wings since the possible presence of brick powder might indicate an incorrect measurement
166 biased by the hit unit. To conclude, the overall procedure of TPT is characterised by specific working stages
167 and subsequent checks that provide a robust and standardized practice to avoid operation errors.

168



169

170 Figure 4 - Analogic torque wrench used for the Torque Penetrometric Test in this work (a) and in-situ application (b).

171

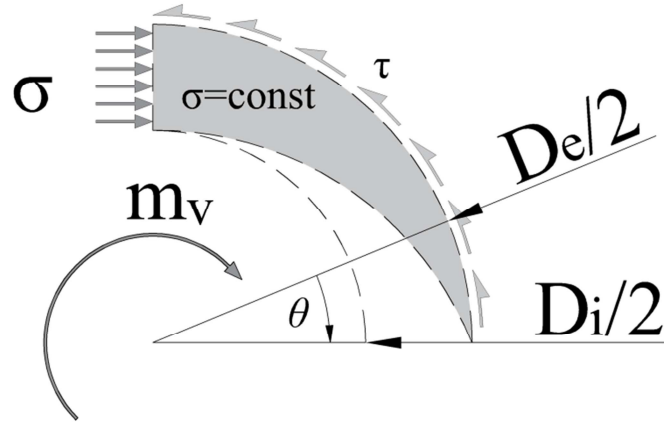
3. Fracture Mechanics Interpretative Theory

This section presents a novel interpretation model for the TPT based on a fracture mechanics theoretical framework. The model is based on the analysis of the stress state on the fracture surface produced by the toothed nail in the mortar joint, under the hypothesis of no interaction with the brick. Such hypothesis is the result of the careful execution procedure presented in Section 2 and reveals to be acceptable in historical brickwork, where the mortar joints are usually thicker than in modern construction (around 15 mm or even more).

The calibration of the model parameters is carried out by considering comprehensive sets of experimental data available in the literature for different types of mortar.

3.1. Theoretical interpretation of the failure mechanism

The point of departure of the interpretation of the TPT is the analysis of the equilibrium in a transversal section of the mortar in contact with the toothed nail of the device. Figure 5 shows the stress state acting on one quarter of the volume of mortar being compressed by one of the teeth during the TPT. The application of a torque per unit length m_v induces the development of compression stresses at the contact surface between the nail's tooth and the mortar material. The distribution of these stresses σ is assumed uniform at failure and with constant magnitude. The shear stresses τ at failure are also assumed constant and uniformly distributed along the external circumference with radius $D_e/2$ from the centre of the toothed nail. The loaded cross section of the mortar volume changes linearly with the angular coordinate θ , as well as the magnitude of the shear action on mortar developed by the torque. Both these two variations change with the same rate and thus the compressive stress acting on mortar is constant regardless of the angular coordinate θ of the cross section of the mortar volume between two consecutive teeth (see Figure 5).



194

195 Figure 5 – Stress state in one quarter of the volume of mortar investigated during the Torque Penetrometric Test.

196

197 On the basis of the presented hypotheses, it is possible to define the elastic strain energy per length unit j_V on
 198 one quarter of the volume of mortar loaded during the TPT, as reported in Equation 1:

$$199 \quad j_V = \int \frac{\sigma^2}{2E} dV = \frac{\sigma^2}{2E} \cdot \frac{\pi \cdot (D_e^2 - D_i^2)}{32} \quad (1)$$

200 where σ is the compression on the tooth (assumed constant), E is the Young's modulus of mortar, D_e is the
 201 external diameter of the toothed part of the nail and D_i is the diameter of the smooth shank.

202 The energy is dissipated through the circumferential slip surface of diameter D_e according to a constant
 203 distribution of tangential stresses only [22]. The main reason that allow disregarding the normal stresses is the
 204 execution of the pilot hole. In fact, the drill removes a cylinder of mortar thus relaxing the radial stresses around
 205 the hole into which the TPT is inserted.

206 The specific energy per length unit j_S on one quarter of the circumferential slip surface is directly related to the
 207 fracture energy of the material G_f , as reported in Equation 2:

$$208 \quad j_S = G_f \cdot \frac{\pi \cdot D_e}{4} \quad (2)$$

209 The two energies calculated in Equations 1-2 must be equivalent, thus it is possible to obtain an expression of
 210 the compression stress on the teeth as reported in Equation 3:

$$\sigma = \sqrt{\frac{16 \cdot E \cdot G_f \cdot D_e}{(D_e^2 - D_i^2)}} \quad (3)$$

The total compression stresses acting over the four teeth of the TPT are in equilibrium with the external torque applied to the instrument (see Figure 5), so they turn out to be:

$$\sigma = \frac{2 \cdot m_v}{(D_e^2 - D_i^2)} \quad (4)$$

The simple equivalence of Equations 3-4 provides a direct relationship between the torque per unit length m_v recorded during the TPT and the mechanical parameters of mortar E and G_f :

$$\frac{2 \cdot m_v}{D_e^2 - D_i^2} = \sqrt{\frac{16 \cdot E \cdot G_f \cdot D_e}{(D_e^2 - D_i^2)}} \quad (5)$$

In analogy with relevant concrete guidelines [23], it is possible to establish regression expressions, relating the Young's modulus E and fracture energy G_f with the compressive strength f_c of mortar material, in the form of simple monomials:

$$E = K_E \cdot \left(\frac{f_c}{f_{c,0}}\right)^\varepsilon ; \quad G_f = K_G \cdot \left(\frac{f_c}{f_{c,0}}\right)^\gamma \quad (6a,b)$$

where the constants K_E , K_G , ε and γ can be defined as the best fit of a large experimental dataset and $f_{c,0} = 1$ MPa is a reference compressive strength. The constants K_E and K_G have the same units of the quantity they are related to (i.e. N/mm² for K_E and mJ/mm² for K_G if SI units are used), whereas ε and γ are non-dimensional.

The introduction of these expressions into Equation 5 defines a direct relationship between the normalised torque m_v measured during the TPT and the compressive strength f_c of the mortar material:

$$f_c = f_{c,0} \cdot \left[\frac{m_v}{2 \cdot \sqrt{K_E \cdot K_G \cdot D_e \cdot (D_e^2 - D_i^2)}} \right]^{\frac{2}{(\gamma + \varepsilon)}} \quad (7)$$

The constants K_E , K_G , ε and γ can be grouped to simplify further the previous expression as follows:

$$f_c = f_{c,0} \cdot \left[\frac{m_v}{2 \cdot \sqrt{K_A \cdot D_e \cdot (D_e^2 - D_i^2)}} \right]^{\frac{2}{\alpha}} \quad (8)$$

where $K_A = K_E \cdot K_G$ and $\alpha = \varepsilon + \gamma$. The term into the square brackets of Equation 8 is non-dimensional. Equation 8 relates the normalised torque m_v measured during the TPT with the compressive strength of the mortar. The

parameters K_A and α establishing such relationship can be calibrated as shown in the next section, by using suitable experimental datasets available in the scientific literature [23–29].

3.2. Calibration of the Model Parameters

The parameters K_E , K_G , ε , γ of Equations 6-7 have to be carefully defined in order to ensure the accuracy of the interpretative theory for the TPT. The values of K_A and α of Equation 8 can be determined through appropriate relationships between the compressive strength of mortar and other mechanical parameters, i.e. Young's modulus and fracture energy.

The first stage of the calibration the model concerns the parameters K_E and ε . Existing standards and experimental studies in the existing literature [23,24,26,30] propose suitable relationships between the Young's modulus and the compressive strength of the material, with expressions very similar to the Equation 6a. Available standards for concrete [23,24] suggest rather low values of ε (respectively 0.33 and 0.30) and high values of K_E (respectively 15100 and 22000). For the specific case of mortars, these values of the parameters lead to an overestimation of the elastic modulus. For this reason, they need to be calibrated in order to cover the representative ranges of compressive strengths of lime or lime-cement mortars [8,9,31,32]. According to all the aforementioned references, realistic values of Young's moduli for historical mortar types are between 500 MPa and 5000 MPa for mortars characterized by compressive strengths in the range between 1.0 MPa to 10.0 MPa [31–34]. The data fit procedure of the whole considered sample of experimental data provides $\varepsilon = 0.7$ and $K_E = 550$ MPa (see Figure 6) with very good agreement with the experimental results ($R^2 = 0.697$).

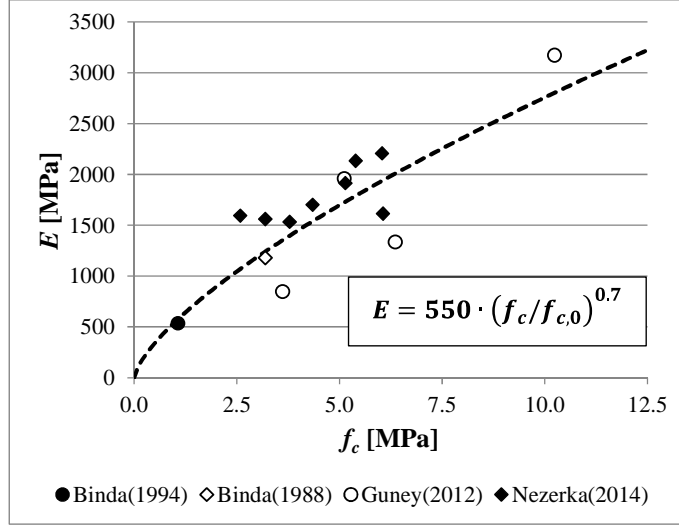


Figure 6 – Empirical relationship between the compressive strength f_c and the Young's Modulus E for different types of mortar ($R^2 = 0.697$) [31–34].

The second stage of the calibration of the model concerns the parameters K_G and γ . Their evaluations require the definition of a suitable relationship between the tangential stress τ and the shear slip s . If this law presents a linear ascending branch followed by linear softening, the area underneath the τ - s diagram can be conventionally quantified by the mode II fracture energy of the material $G_{f,II}$. If a simple bilinear relationship between τ and s is considered for the mortar material, the mode II fracture energy can be expressed as follows:

$$G_{f,II} = \frac{\tau_{max}^2}{2K_0} \mu, \quad (9)$$

where K_0 is the elastic stiffness of the fracturing shear interface, and μ is the ductility factor expressing the ultimate slip s_u as a function of the slip s_0 at the maximum tangential stress τ_{max} .

If the compression stress is small, as in the case of historical mortars, and under the hypothesis of associate plastic flow rule [22], the maximum tangential stress can be assumed as the cohesion of the material according to the Coulomb failure model:

$$\tau_{max} = \frac{1}{2} \sqrt{f_c f_t}, \quad (10)$$

where f_c and f_t are the uniaxial compressive and tensile strengths of the mortar. By substituting Equation 10 into Equation 9, the fracture energy can be defined as a function of both the strengths f_c and f_t . Such relationship can

270 be further simplified by expressing the tensile strength as a function of the compressive one, as it is usual in the
271 existing literature [24,26]:

$$272 \quad f_t = K_t \left(\frac{f_c}{f_{c,0}} \right)^\beta \quad (11)$$

273 Where the K_t and β parameters can be evaluated empirically from available experimental datasets. References
274 [24,26] suggests K_t in the range 0.20 to 0.40, and β in the range 0.70 to 1.0. The reference compressive strength
275 can be assumed $f_{c,0} = 1$ MPa as in Equations 6-8.

276 Available experimental studies normally relate the compressive strength of the mortar with its flexural strength
277 f_{ft} instead of the tensile one. This is due to the intrinsic difficulties related to the execution of direct tensile tests.
278 The available standard for mortar materials actually recommends the development of flexural tests [35]. The
279 flexural strength can be converted to the tensile one using a reduction factor that assumes different values
280 depending on the specific standard. According to [23,24,30], if the standard $40 \times 40 \times 160$ mm³ specimens are
281 considered for the flexural tests of mortar, the ratio between tensile and flexural strengths is in the range 0.44 to
282 0.83. In almost all the aforementioned references, the correlation proposed between f_t and f_{ft} is linear. Therefore,
283 it is possible to define the relationship between the compressive and flexural strengths by using a suitable value
284 of the parameter K_{ft}

$$285 \quad f_{ft} = K_{ft} \left(\frac{f_c}{f_{c,0}} \right)^\beta \quad (12)$$

286 The constant K_{ft} and the exponent β of Equation 12 can be obtained by a data fit procedure of available
287 experimental data [10,14,25,26,36], specific to the type of weak historical mortars that are considered in the
288 present study. The performed identification yields for the cited parameters values of 0.60 MPa and 0.75, with
289 an R^2 of 0.866 (see Figure 7). The K_t parameter of Equation 11 can be thus assumed equal to 0.38 MPa, i.e. to
290 the mean value of the interval 0.25 – 0.50 MPa that emerges from the experimental data transformed to direct
291 tensile strength [24].

292

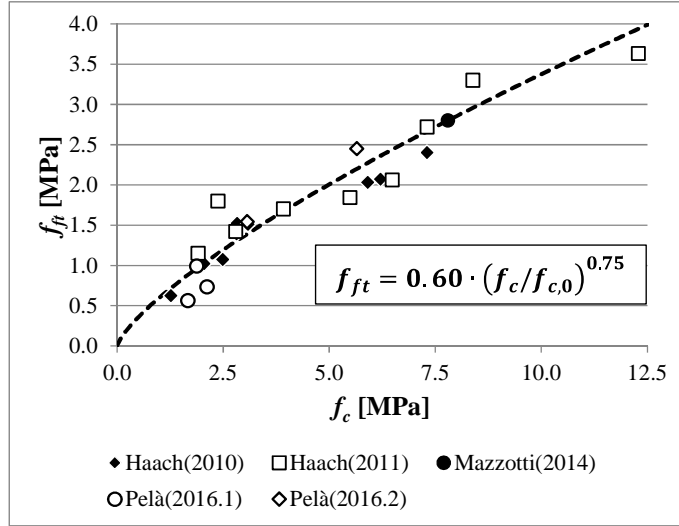


Figure 7 - Empirical relationship between the compressive strength f_c and the flexural strength f_{ft} for different types of mortar ($R^2 = 0.866$) [10,14,25,26,36].

The elastic stiffness of the fracturing shear interface K_0 in Equation 9 is very difficult to be evaluated, since it is related to the characteristic length of the fracture process. An approximation based on the hypotheses of linear elastic – linearly softening brittle material [37] provides the following expression:

$$G_{F,II} = \frac{\sqrt{K_t f_{c,0}}}{4} s_u \left(\frac{f_c}{f_{c,0}} \right)^{\frac{1+\beta}{2}} \quad (13)$$

The ultimate slip s_u of the mode II fracture is almost independent of both the type of experimental set up and the material strength [27,29,38,39] and it can be assumed ranging between 0.5 mm and 1.0 mm, with lower values holding for stiffer and stronger mortars. The fracture energy can be thus expressed in the form of Equation 6b by considering the following definitions of the corresponding parameters:

$$K_G = \frac{\sqrt{K_t f_{c,0}}}{4} s_u, \quad \gamma = \frac{1+\beta}{2} \quad (14a,b)$$

The mode II fracture energy is a debated parameter and its experimental determination is not straightforward. Available studies [29,40] show that mode II and mode III fracture energies have a well-defined ratio to mode I values obtained by means of different experimental methods. Reference [38] provides a mode II fracture energy of 100 J/m² for weak and strong mortar at a confining pressure of 500 kPa. Reference [39] provides characteristic values for tuff masonry in shear of 120-170 J/m² for a compressive strength of 2.5 MPa. Representative values of mode I fracture energy of mortar are in the range 5-10 J/m² in available studies

312 [27,38,41]. Thus, realistic values of mode II fracture energy for typical historical mortar can be defined in the
 313 range between 100 J/m² and 200 J/m², whilst ordinary cementitious mortars might reach upper bound values
 314 around 400 J/m² [37, 40].

315 The parameter K_G can be evaluated by introducing suitable values of K_t and s_{it} . As indicated before, K_t can be
 316 assumed equal to 0.38 MPa and the ultimate slip can range between 0.5 mm and 1.0 mm [27,29,38,39]. Thus,
 317 the K_G parameter can range between 80 J/m² and 150 J/m² (Equation 14a), depending on the assumed value of
 318 the ultimate slip. Smaller K_G values should be referred to stiffer mortars, which exhibit shorter slips. For
 319 example, if the mortar compressive strength is within the interval 1.0 ÷ 3.0 MPa, the corresponding range of
 320 mode II fracture energy can be evaluated in the interval 150 ÷ 210 J/m², i.e. in good agreement with the
 321 experimental results from the literature.

322 On the basis of the previous considerations, a realistic value for K_G can be set around 0.10 mJ/mm².
 323 Considering the parameter β equal to 0.75, as discussed above, the γ exponent results equal to 0.87 according to
 324 Equation 14b. All these values, inserted into Equation 6b, approximate rather well the parameters of the
 325 experimental dataset. Hence, $K_A = K_E \cdot K_G = 0.10 \cdot 550 = 55 \text{ N}^2/\text{mm}^3$ and $\alpha = \epsilon + \gamma = 0.7 + 0.87 = 1.57$.

326 The calibration of the model parameters leads finally to the analytical expression relating the compressive
 327 strength of the material to the maximum normalized torque measured during the TPT:

$$328 \quad f_c = \left[\frac{m_v}{2 \cdot \sqrt{55 \cdot D_e \cdot (D_e^2 - D_i^2)}} \right]^{1.274}, \quad (15)$$

329 Where f_c is expressed in [MPa], m_v in [Nmm/mm], and D_e and D_i in [mm].

330 Since the error in the evaluation of K_E and K_G from experimental data has resulted in 16% approximately, the
 331 error in the TPT estimation of f_c can be supposed to be around $\sqrt{0.16^2 + 0.16^2} = 0.226$, i.e. 23%.

332 **4. Experimental validation of the Fracture Mechanics interpretative** 333 **theory**

334 This section presents the experimental validation of the novel interpretative theory for the TPT. The calibration
335 of the procedure was carried out by considering an experimental program developed by the authors [7,21] as
336 well as the data from an additional campaign available in the literature [20]. The practical application of the
337 TPT and the validation of the interpretative theory are eventually presented with reference to experiments on a
338 masonry wall built in the laboratory with historical-like materials [9,10] and on the existing masonry walls of
339 an historical building struck by the 2012 Emilia-Romagna earthquake.

341 **4.1. Calibration of TPT through the experimental programs at UNIBO and DTI**

342 The calibration of the instrument was carried out by comparing the standard compressive strengths obtained
343 from standard laboratory tests with maximum torque values measured with the TPT [7,21] and the X-Drill [20].
344 The two experimental programs were carried out respectively at the University of Bologna (UNIBO) by the
345 present authors and at the Danish Technological Institute (DTI) by Christiansen. All the experimental data are
346 reported for sake of completeness in the Annexes A.1 and A.2.

347 The experimental program at UNIBO consisted in comparing the maximum torque measured during the TPT
348 with the standard compressive strength obtained from laboratory tests. A rigorous way to compare these two
349 parameters is to perform both the tests directly on the same specimen. In order to limit the influence of the
350 minor damage induced by the TPT test, the compression tests were carried out by loading the same faces where
351 the penetrometric tests were performed. In this way, the part of the specimen damaged by the TPT was located
352 next to the loading plates, i.e. in the most confined part of the sample during the compression test. The current
353 standard for the mechanical characterisation of mortar [42] requires prismatic samples with nominal dimensions
354 $40 \times 40 \times 160 \text{ mm}^3$. However, the small dimensions of these specimens would not permit the execution of the
355 torque tests, causing an early collapse of the specimen and also avoiding the possibility to test it subsequently in
356 compression. For this reason, bigger cubic specimens were chosen for the calibration of the tool, using the

357 standard for concrete materials as reference [43]. TPT was executed twice on each sample. The specimen was
358 firstly placed between the platens of a loading machine under a constant compression of 2 kN, owing to avoid
359 any movement of the specimen during the torque test. However, the X-Drill investigation by Christiansen [20]
360 showed that the vertical stress does not influence the test results. Once the sample was fixed between the plates,
361 the nail was knocked into the pilot hole using a hammer until its toothed part was completely inserted, see
362 Figure 8.

363 The testing operation proceeded with the application of a torque on the inserted toothed nail. This operation was
364 carried out using the torque wrench, recording for each test the maximum measured value of the torque. The
365 torque wrench must be handled with some caution in order to avoid any transversal force that could affect the
366 test and lead to an erroneous evaluation of the maximum torque.



367
368 Figure 8 - Mortar sample with the inserted toothed nail ready for the torque test

369
370 The subsequent stage of the experimental program consisted in the compression tests of the cubic specimens.
371 Each sample was placed with the damaged faces in direct contact with the loading platens of the compression
372 machine. The peak stress recorded during each experiment was regarded as the compressive strength of the
373 tested mortar specimen.

374 The experimental program at DTI was also based on the comparison between the maximum torques measured
375 with the X-Drill device and the standard compressive strengths obtained from laboratory tests. This second
376 experimental program was considered in extending the database of TPT results obtained at UNIBO. However,

377 X-Drill original measurements data had to be adjusted in order to make possible a direct comparison with the
378 TPT results, since the two penetrometers have different geometries. In particular, the measured ultimate torque
379 is strictly dependent on the fracture surface activated by the tools. The TPT and the X-Drill provide different
380 readings of the maximum torque if executed over the same material, because their toothed nails have different
381 areas in contact with the investigated material. The values of the internal and external diameters of the toothed
382 part of the nail D_i and D_e are different in the two instruments: $D_i=7$ mm and $D_e=9$ mm for the TPT whereas
383 $D_i=6.5$ mm and $D_e=10$ mm for the Christiansen's X-Drill. For this reason, the original readings from the X-
384 Drill campaign at DTI were properly adjusted in order to make them directly comparable to those obtained with
385 TPT. Using Equation 4, the following expression was adopted to convert the original normalised ultimate
386 torques measured with X-Drill $m_{v,XDrill}$ to their adjusted values $m_{v,TPT}$ comparable with TPT:

$$387 \quad m_{v,TPT} = \frac{\left[\sqrt{(D_e^2 - D_i^2) D_e} \right]_{TPT}}{\left[\sqrt{(D_e^2 - D_i^2) D_e} \right]_{XDrill}} m_{v,XDrill} = 0.706 m_{v,XDrill} \quad (16)$$

388 Figure 8 shows the adjusted data $m_{v,TPT}$ from the DTI tests together with the TPT data from the UNIBO
389 experiments, all related to the corresponding standard strengths of the investigated mortars. The data fitting was
390 carried out by using a least square algorithm where the two variables are the parameters K_A and α of Equation
391 8. This methodology provided the values $K_A = 54$ and $\alpha = 1.53$ with high coefficient of determination $R^2 =$
392 0.96. Moreover, those parameters are very close to those suggested in Section 3 for the fracture mechanics
393 interpretative theory of the TPT, showing the correctness of the proposed model.

394

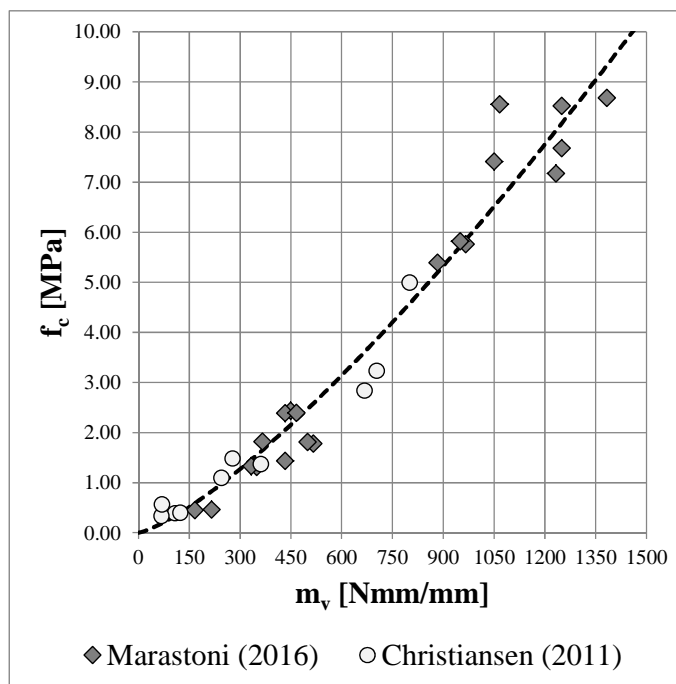


Figure 9 - Empirical correlation between the standard compressive strength of mortar and the measurements made with the torque penetrometer tests developed at UNIBO [7,21] and the X-Drill tests developed at DTI [20].

4.2. TPT applied to a Replicated Historical-Like Wall built at UPC

The TPT was used to perform experiments on a wall built in the Laboratory of Technology of Structures and Materials (LATEM) of the Technical University of Catalonia (UPC-BarcelonaTech), Spain.

The lime mortar and bricks used for the construction of this wall were chosen in order to simulate a handmade historical masonry structural panel. The dimensions of the brick units were $275 \times 135 \times 45 \text{ mm}^3$. The mortar was mixed starting from the raw components, using fine river sand with $0 \div 2 \text{ mm}$ grain size. Natural hydraulic lime NHL 3.5 was utilized with volume ratio of binder to aggregate of 1:3, which is rather typical in the traditional manufacturing of mortar in masonry construction [30,44].

Using the aforementioned components, a wall with rough dimensions $1.50 \times 0.75 \times 0.275 \text{ m}^3$ was built in Flemish bond (see Figure 10). The external thickness of the joints was variable, from 10 mm to 15 mm, due to the imperfect faces of the handmade bricks. The wall was stored in the laboratory for 110 days, i.e. until when mortar had reached a sufficient strength in order to replicate the property of a historical masonry.

412



413

414 Figure 10 - Construction stage (a) and the wall at the end of the construction (b).

415

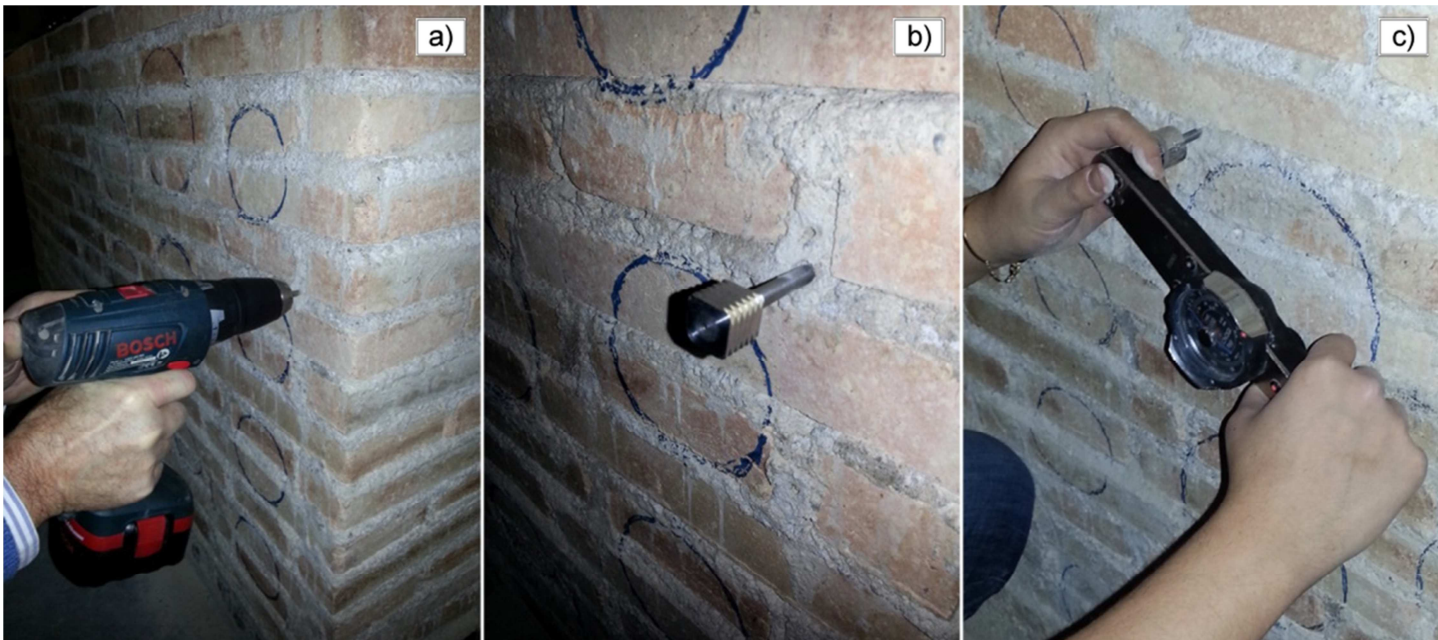
416 During the construction of the wall, the mortar was characterised according to the EN 1015-11:2007 procedure
417 [35]. Standard samples were prepared using the same mortar utilised in the wall construction, allowing a
418 complete characterisation of the material in tension and compression. Three $40 \times 40 \times 160 \text{ mm}^3$ prisms were
419 tested 110 days after their construction to determine the flexural strength f_{ft} , whereas the compressive strength f_c
420 was assessed on the six halves produced by the splitting of the prisms from the flexure tests.

421 The average value of the flexural strength was 0.38 MPa with a coefficient of variation (CV) of 6%. The
422 compression tests were performed on the six fragments produced by the flexural tests. The two stumps
423 measured roughly $40 \times 40 \times 80 \text{ mm}^3$ and were loaded with steel loading platens of $40 \times 40 \text{ mm}^2$. The average
424 compressive strength was 2.79 MPa with a CV of 9%.

425 The operational sequence used in carrying out the TPT tests was intended to reproduce a generic in-situ activity
426 on existing walls. The penetrometric tests were performed in random positions on the masonry wall, in order to
427 provide globally representative results. The pilot holes were performed using a portable driller equipped with a
428 7 mm bit made of hardened steel, carefully checking the orthogonality of the hole to the external surface of the
429 wall (Figure 11a). Once the pilot holes were properly made, the nail was hammered into each hole (Figure 11b)

430 and the TPT was executed using the torque wrench (Figure 11c). The resulting moments measured in 12
 431 positions are reported in Table 1.

432



433

434 Figure 11 - Execution of the pilot hole on the wall (a), toothed nail inserted into the mortar joint (b) and test execution using the
 435 torque wrench (c).

436

437 Table 1 - Experimental results of the penetrometric tests performed on the wall.

Test	M_v [Nm]	m_v [Nmm/mm]	Test	M_v [Nm]	m_v [Nmm/mm]
TPT01	6.5	433	TPT07	10.0	667
TPT02	8.0	533	TPT08	10.0	667
TPT03	10.0	667	TPT09	8.0	533
TPT04	7.5	500	TPT10	9.0	600
TPT05	7.0	467	TPT11	7.5	500
TPT06	9.5	633	TPT12	7.5	500
			Avg.	8.4	558
			CV	15%	15%

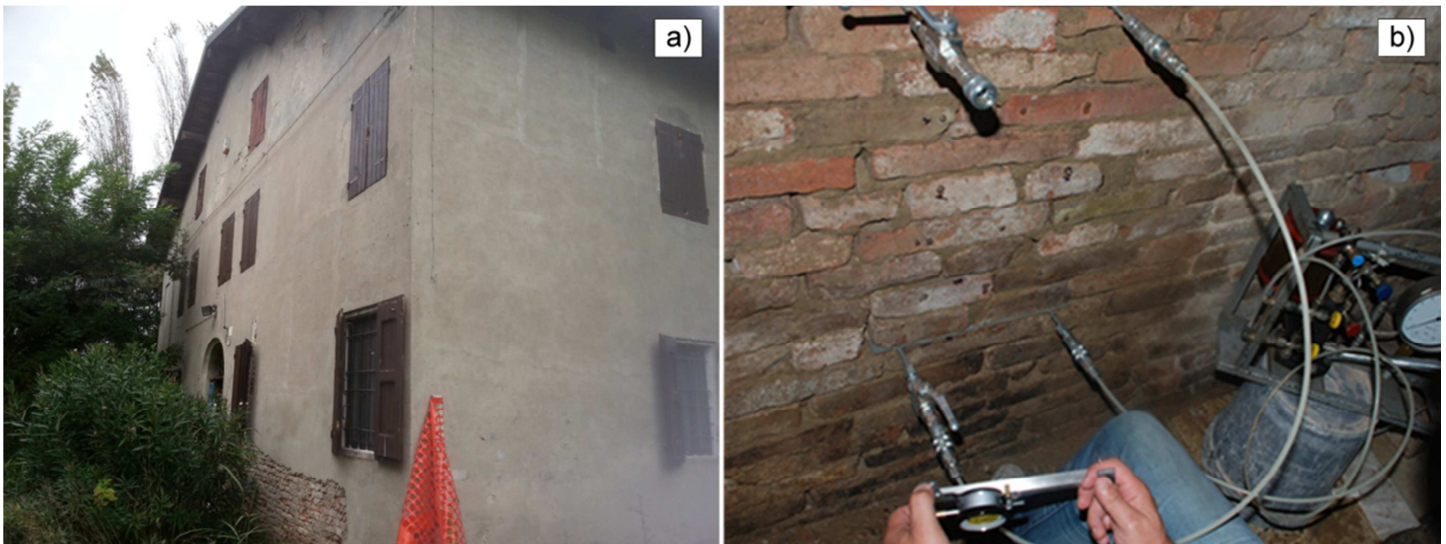
438

439 The average value obtained by the experimental testing with the latest tool geometry was $M_v=8.4$ Nm with a
 440 CV of 15%. The specific ultimate torque related to the aforementioned average value is $m_v=558$ Nmm/mm.
 441 Equation 15 can be used for the estimation of the mortar strength, providing a value of the compressive strength
 442 of 2.87 MPa. There is only a 3% difference between the actual compressive strength obtained in the mechanical
 443 characterisation and its estimated value with TPT. This low difference between the standard compression test
 444 results and the evaluation from the penetrometric readings suggests the reliability of the methodology proposed,
 445 returning low scattered results (CV=15%) and a good precision in the prediction of the compressive strength of
 446 mortar.

447

448 **4.3. TPT applied to a Historical Masonry Building**

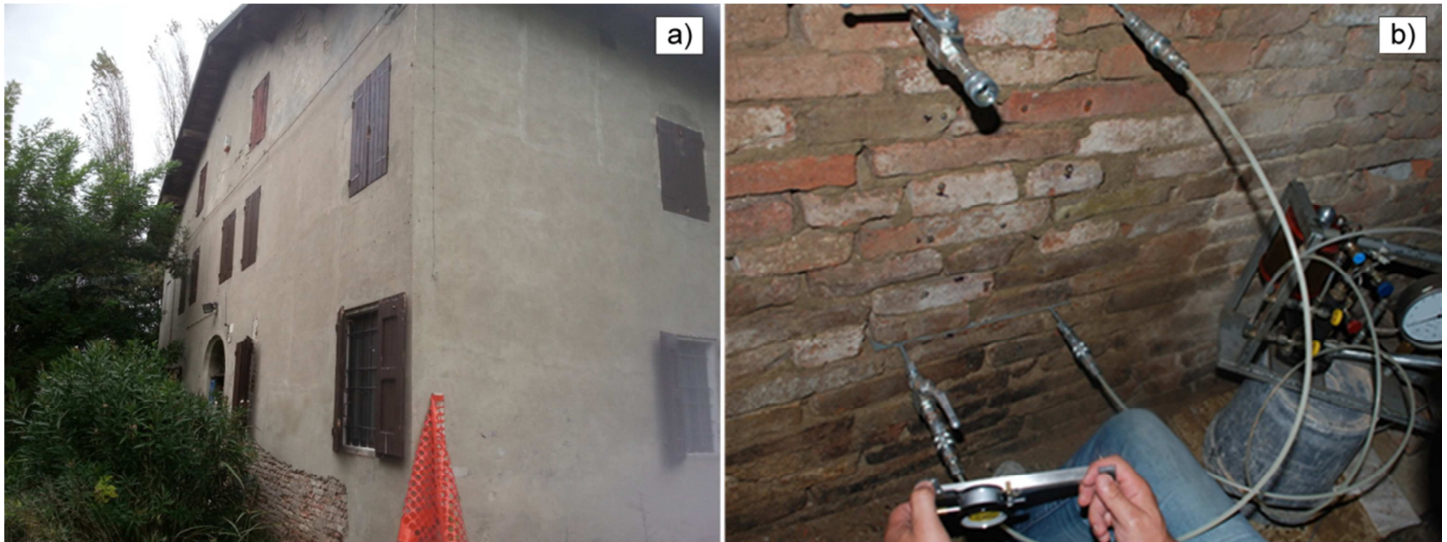
449 The TPT was executed during an experimental campaign carried out on a 19th century rural masonry building,
 450 called “Leona”, located in the countryside of the town of Cento, in the province of Ferrara, Italy. The building
 451 was damaged by the 2012 Emilia Earthquake (see



452

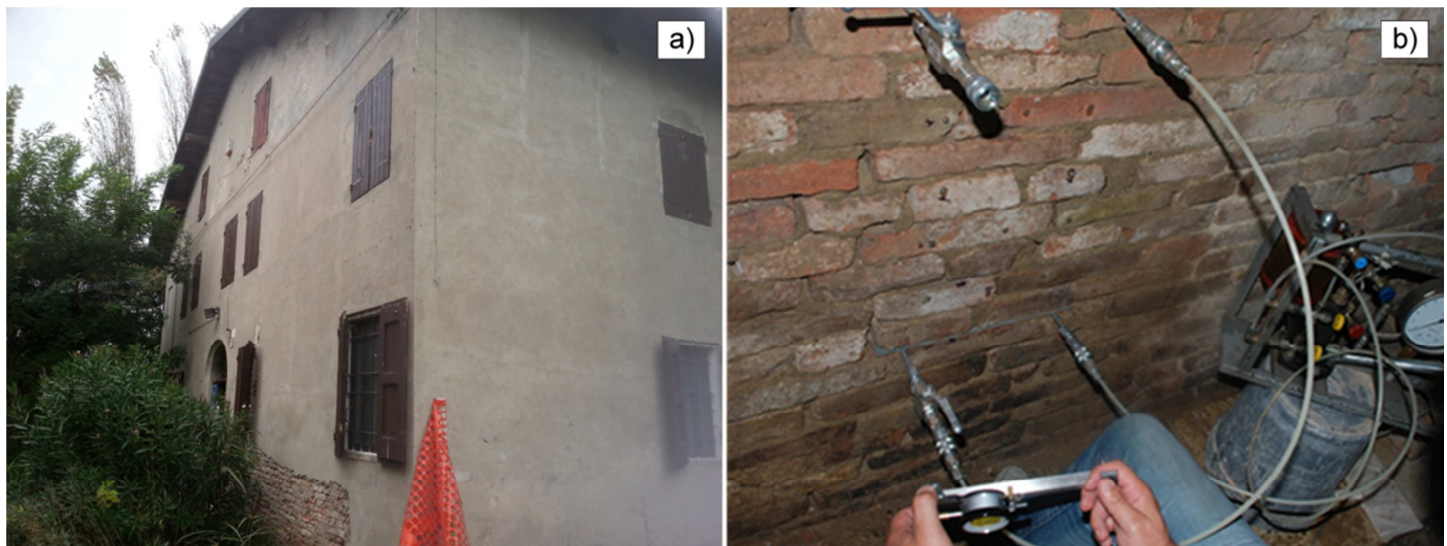
453 Figure 12a), as well as most of the rural structures of the area, due to the very poor materials employed in the
 454 construction. The inspection and the analysis of the damage suffered by Leona building were supported by an
 455 experimental campaign focusing on the assessment of the material mechanical properties, as an essential issue
 456 in planning the necessary repair and retrofit interventions.

457 The experimental program consisted in the execution of a sequence of increasingly destructive types of tests.
458 As usual, during the inspection of existing historical structures, the first analyses were carried out using MDT
459 techniques in order to limit the damage induced to the structural members. The TPT was performed to get a
460 quick in-situ assessment of the strength of mortar in the joints. Afterwards, mortar joint samples were extracted
461 from the existing brickwork, taking advantage of zones with disjointed bricks or cracks, and then subjected to
462 double punch test (DPT) in the laboratory [7,8,45,46] . Finally, on site destructive tests were carried out using
463 the double flat jack (DFJ) in order to obtain a direct evaluation of the masonry strength (



464
465 Figure 12b).

466 The TPT and DPT were executed in four different positions on the structure in order to evaluate the spatial
467 variability of the properties of the materials in the Leona building. DFJ was carried out only in two positions.
468 The correlation of accurate and expensive investigation techniques with cheaper and faster MDT evaluations
469 can draw information about the spatial variability of the mechanical properties on the same building. By this
470 way, different construction techniques, building ages, conservation levels and damage severities can be detected
471 and distinguished.



472
473 Figure 12 - External view of Leona Building in Cento (Ferrara, Italy) (a) and double flat jack executed on an external wall (b).
474

475 Table 2 presents a summary of all the results obtained from the different experiments carried out on the
476 different positions of Leona building.

477 The TPT readings were twelve for each one of four selected positions. As shown, the estimations of the mortar
478 compressive strengths measured in the four different positions ranged between 0.49 MPa and 1.16 MPa.

479 Four mortar samples for each selected position were subjected to DPT in the laboratory. As reported in previous
480 researches available in the literature [7,8,45–48], the ultimate load obtained from the DPT cannot be considered
481 equal to the uniaxial compressive strength of the material due to the confinement pressure exerted by the
482 loading plates on the thin mortar specimen. The conversion between the DPT and the uniaxial compressive
483 strengths can be evaluated by applying the correction factor of 0.7 proposed by [46], leading to the average
484 compressive strengths for each position reported in Table 2.

485 The DFJ tests provided very low values of the compressive strength (0.52 MPa and 0.82 MPa). These results
486 showed clearly that the failure of masonry, under this compression setup, occurred entirely in the mortar joint
487 due to local crushing. This type of response constituted a further evidence of the poor properties of the
488 investigated mortar, as usual in the rural construction of the region. Therefore, the compressive strength values
489 derived from the DFJ could be compared with the DPT results and the TPT readings performed in the same
490 positions.

491 Table 2 shows the comparison among the predictions from the different experimental techniques. TPT
 492 estimations of the mortar compressive strength are in remarkable agreement with those provided by other
 493 consolidated testing methods (DPT and DFJ). The highest error of the TPT of -27%, obtained in the Position 2,
 494 was probably due to the testing of mortar in a more superficial position than DPT and DFJ. Overall, the good
 495 agreement highlights the validity of the calibration presented in this paper for the TPT technique. In addition,
 496 the TPT showed its capability to detect the variability of the mechanical properties for different positions of the
 497 building with a very good precision and with acceptable scattering of the obtained measures.

498
 499 Table 2 - Comparison of the different experimental predictions of mortar compressive strength.

Test	Pos. 1 [MPa]	Pos. 2 [MPa]	Pos. 3 [MPa]	Pos. 4 [MPa]
TPT	0,49	0,54	0,91	1,16
DPT	0,55	0,86	0,94	0,90
DFJ	0,52	0,82		
Average	0,52	0,74	0,93	1,03
TPT Error	-6%	-27%	-2%	+13%

500
 501 **5. Conclusions**

502 This research was developed with the purpose to provide a reliable calibration and an interpretation model for a
 503 new MDT technique, called Torque Penetrometric Test (TPT), developed for a quick in-situ evaluation of the
 504 compressive strength of historical mortars [7,21]. The TPT is a portable apparatus that is characterised by easy
 505 execution and repeatability of measurements. The equipment has only two components, i.e. a steel nail with
 506 four protruding teeth and a torque wrench. This novel instrument is conceptually similar to the geotechnical
 507 testing method of the vane shear test and constitutes an improvement of the previously proposed X-drill method
 508 [20]. The research proposes a specific shape for the toothed nail to be inserted into the mortar joint, making the

509 technique more suitable for the investigation of historical mortars. The proposed enhancements are effective in
510 reducing the uncertainties in the measurements since:

- 511 - the teeth's length $L_w=15$ mm allows for a standardisation of the penetration depth;
- 512 - the shank's diameter of 6.5 mm allows the deep penetration of the nail into the mortar joint without any
513 interaction with the superficial portion of the mortar joint in the wall;
- 514 - the diameter of the toothed head of 9 mm allows inserting it quite easily into most of the existing mortar
515 joints;
- 516 - the peculiar geometry of the toothed nail of the TPT is suitable both for superficial and deep measurements
517 of the strength of the mortar in existing walls.

518 The present research, as a first approach to set up the TPT, has considered a simple analogic torque wrench,
519 even though future applications could use more expensive digital acquisition systems to obtain more accurate
520 estimations as well as continuous measurements of both the torque and twisting angle.

521 An interpretative theory has been proposed by developing a micro-mechanical analysis of the stress state
522 induced by the TPT on the investigated mortar, and also considering basic concepts of fracture mechanics. The
523 presented theory yields a simple analytical expression relating the compressive strength of the mortar with the
524 normalised ultimate torque (maximum torque per unit length) recorded during the TPT. All the parameters of
525 the proposed model have been carefully calibrated making reference to comprehensive experimental datasets
526 available in the literature for mortars with compressive strength within the typical ranges for existing masonry
527 buildings. This activity has allowed the determination of suitable relationships among the Young's modulus, the
528 fracture energy and the compressive strength of different types of mortars.

529 The results obtained from this study can be summarised as follows:

- 530 - the proposed interpretation theory for the TPT has shown a remarkable agreement with the best fit curves
531 defined on the basis of compression and penetrometric experiments developed at the laboratories of UNIBO
532 and DTI. The whole experimental dataset covers a range of mortar compressive strengths from 0.34 MPa to
533 8.55 MPa, proving the applicability of the method to the typical mortar types of historical masonry
534 buildings.

- 535 - the proposed interpretation theory for the TPT has shown to be accurate in predicting the compressive
536 strength of the mortar used in a wall built in the UPC laboratory according to the traditional techniques of
537 historical masonry construction. The completed TPT evaluation has provided a compressive strength almost
538 equal to the standard strength got from direct compression tests.
- 539 - the TPT has been also conducted on a historical masonry building damaged by the 2012 Emilia-Romagna
540 earthquake (Italy). The estimation of the mortar strength provided by the calibrated theory has resulted in a
541 remarkable agreement with values derived from other more consolidated experimental techniques, i.e.
542 double punch tests and double flat jack tests. Moreover, the TPT has showed to be a useful approach for its
543 speed and ease in the in-situ assessment of the mortar strength. This specific feature of the TPT makes it
544 appropriate for historical structures of the built heritage with medium to poor material properties. The TPT
545 has shown also to be a suitable complement to more invasive testing methods, such as the double flat jack
546 test and the double punch test, allowing to plan more efficient experimental campaigns on historical
547 masonry buildings.
- 548 - The interpretative theory proposed in this paper for TPT constitutes a very helpful tool to improve the
549 understanding and post-processing of experimental results. The average error recorded in the experimental
550 investigations (10% – 15%) is lower than the theoretical error (23%).

Acknowledgements

This research has received the financial support from the ReLUIS 2013 research program (Theme 2 – Line 3 – Task 1: Analysis and Development of New Materials for Seismic Retrofit) granted by the DPC – Civil Protection Agency, and from the MINECO (Ministerio de Economía y Competitividad of the Spanish Government) and the ERDF (European Regional Development Fund) through the MULTIMAS project (Multiscale techniques for the experimental and numerical analysis of the reliability of masonry structures, ref. num. BIA2015-63882-P). Diego Marastoni acknowledges the University of Bologna and the SPINNER Consortium for granting his PhD scholarship. Benedetti&Partners consulting is also gratefully acknowledged for making available the experimental results carried out in Cento (FE), Italy.

References

- [1] H. Kaplan, H. Bilgin, S. Yilmaz, H. Binici, A. Öztas, Structural damages of L’Aquila (Italy) earthquake, *Nat. Hazards Earth Syst. Sci.* 10 (2010) 499–507. doi:10.5194/nhess-10-499-2010.
- [2] N. Augenti, F. Parisi, Learning from Construction Failures due to the 2009 L’Aquila, Italy, Earthquake, *J. Perform. Constr. Facil.* 24 (2010) 536–555. doi:10.1061/(ASCE)CF.1943-5509.0000122.
- [3] ISCARSAH, Recommendations for the analysis, conservation and structural restoration of Architectural Heritage, *Int. Council. Monum. Sites.* (2003).
- [4] D.. McCann, M.. Forde, Review of NDT methods in the assessment of concrete and masonry structures, *NDT E Int.* 34 (2001) 71–84. doi:10.1016/S0963-8695(00)00032-3.
- [5] EN 1998-3:2013, Eurocode 8: Design of structures for earthquake resistance - Part 3: Assessment and retrofitting of buildings, (2013).
- [6] V. Bosiljkov, M. Uranjek, R. Žarnić, V. Bokan-Bosiljkov, An integrated diagnostic approach for the assessment of historic masonry structures, *J. Cult. Herit.* 11 (2010) 239–249. doi:10.1016/j.culher.2009.11.007.
- [7] D. Marastoni, Advanced Minor Destructive Testing for the Assessment of Existing Masonry, University of Bologna, available at: <http://amsdottorato.unibo.it/id/eprint/7391>, 2016. <http://amsdottorato.unibo.it/id/eprint/7391>.
- [8] D. Marastoni, L. Pelà, A. Benedetti, P. Roca, Combining Brazilian tests on masonry cores and double punch tests for the mechanical characterization of historical mortars, *Constr. Build. Mater.* 112 (2016) 112–127. doi:10.1016/j.conbuildmat.2016.02.168.

- 578 [9] L. Pelà, E. Canella, A. Aprile, P. Roca, Compression test of masonry core samples extracted from existing brickwork, *Constr.*
579 *Build. Mater.* 119 (2016) 230–240. doi:10.1016/j.conbuildmat.2016.05.057.
- 580 [10] L. Pelà, P. Roca, A. Benedetti, Mechanical Characterization of Historical Masonry by Core Drilling and Testing of
581 Cylindrical Samples, *Int. J. Archit. Herit.* 10 (2016) 360–374. doi:10.1080/15583058.2015.1077906.
- 582 [11] L. Pelà, K. Kasioumi, P. Roca, Experimental evaluation of the shear strength of aerial lime mortar brickwork by standard tests
583 on triplets and non-standard tests on core samples, *136 (2017) 441–453.* doi:10.1016/j.engstruct.2017.01.028.
- 584 [12] L. Pelà, P. Roca, A. Aprile, Combined in-situ and laboratory minor destructive testing of historical mortars, *Int. J. Archit.*
585 *Herit.* DOI: 10.1080/15583058.2017.1323247 (2017).
- 586 [13] ASTM C803, Standard Test Method for Penetration Resistance of Hardened Concrete, *ASTM Int.* (2010).
- 587 [14] L. Pelà, P. Roca, A. Aprile, Comparison of MDT techniques for mechanical characterization of historical masonry, in: Van
588 Balen, Verstrynghe (Eds.), *Proc. 10th Int. Conf. Struct. Anal. Hist. Constr.*, Taylor & Francis, Leuven, Belgium, 2016: pp.
589 769–775.
- 590 [15] EN 12504-2:2012, Testing concrete in structures - Part 2: Non-destructive testing. Determination of rebound number, (2012).
- 591 [16] L.J.A.R. Van Der Klugt, The pointing hardness tester - an instrument to meet a need, *Mater. Struct.* 24 (1991) 471–476.
- 592 [17] R. Nogueira, A.P. Ferreira Pinto, A. Gomes, Assessing mechanical behavior and heterogeneity of low-strength mortars by the
593 drilling resistance method, *Constr. Build. Mater.* 68 (2014) 757–768. doi:10.1016/j.conbuildmat.2014.07.010.
- 594 [18] R. Felicetti, N. Gattesco, A penetration test to study the mechanical response of mortar in ancient masonry buildings, *Mater.*
595 *Struct.* 31 (1998) 350–356. doi:10.1007/BF02480678.
- 596 [19] D. Liberatore, N. Masini, L. Sorrentino, V. Racina, M. Sileo, O. AlShawa, L. Frezza, Static penetration test for historical
597 masonry mortar, *Constr. Build. Mater.* 122 (2016) 810–822. doi:10.1016/j.conbuildmat.2016.07.097.
- 598 [20] P.D.V. Christiansen, In Situ Determination of the Compressive Strength of Mortar Joints Using an X-Drill, *Mason. Int.*
599 (2011).
- 600 [21] D. Marastoni, A. Benedetti, L. Pelà, Evaluation of mortar strength in existing masonry structures through a Minor Destructive
601 Technique, in: C. Modena, F. da Porto, M.R. Valluzzi (Eds.), *Brick Block Mason.*, CRC Press, Padova, Italy, 2016: pp. 1699–
602 1706. doi:10.1201/b21889-225.
- 603 [22] W.-F. Chen, D.-J. Han, *Plasticity for Structural Engineers*, Springer-Verlag New York Inc., New York, USA, 1988.
- 604 [23] fib, *fib Model Code for Concrete Structures 2010*, Wiley-VCH Verlag GmbH & Co. KGaA, Weinheim, Germany, 2013.
605 doi:10.1002/9783433604090.
- 606 [24] EN 1992-1-1:2005, Eurocode 2: Design of concrete structures - Part 1-1: General rules and rules for buildings, (2005).
- 607 [25] V.G. Haach, G. Vasconcelos, P.B. Lourenço, G. Mohamad, Influence of the mortar on the compressive behavior of concrete
608 masonry prisms, *Mecânica Exp.* 18 (2010) 79–84. http://www-ext.lnec.pt/APAET/pdf/Rev_18_A9.pdf.

- 609 [26] V.G. Haach, G. Vasconcelos, P.B. Lourenço, Influence of aggregates grading and water/cement ratio in workability and
610 hardened properties of mortars, *Constr. Build. Mater.* 25 (2011) 2980–2987. doi:10.1016/j.conbuildmat.2010.11.011.
- 611 [27] R. Van Der Pluijm, H. Rutten, M. Ceelen, Shear Behaviour of Bed Joints, in: 12th Int. Brick/Block Mason. Conf., Madrid,
612 Spain, 2000: pp. 1849–1862. <http://www.hms.civil.uminho.pt/ibmac/2000/1849.pdf>.
- 613 [28] H.W. Reinhardt, J. Ošbolt, X. Shilang, A. Dinku, Shear of structural concrete members and pure mode II testing, *Adv. Cem.*
614 *Based Mater.* 5 (1997) 75–85. doi:10.1016/S1065-7355(96)00003-X.
- 615 [29] C.H. Surberg, E.K. Tschegg, Fracture behaviour testing of cementitious interfaces in mode I, II, III, in: R. de Borst, J. Mazars,
616 G. Pijaudier-Cabot, J.G.M. van Mier (Eds.), *Proc. 4th Int. Conf. Fract. Mech. Concr. Concr. Struct.*, A.A. Baklema Publishers,
617 Cachan, France, 2001: pp. 453–460.
- 618 [30] D.M. 14/01/2008, Approvazione delle nuove norme tecniche per le costruzioni, (2008).
- 619 [31] L. Binda, G. Mirabella Roberti, C. Tiraboschi, S. Abbaneo, Measuring Masonry Material Properties, in: D. Abrams, G.M.
620 Calvi (Eds.), *U.S.-Italy Work. Guidel. Seism. Eval. Rehabil. Unreinforced Mason. Build.*, Pavia, Italy, 1994: pp. 326–347.
621 doi:10.1017/CBO9781107415324.004.
- 622 [32] L. Binda, G. Fontana, G. Frigerio, Mechanical behaviour of brick masonries derived from units and mortar characteristics, in:
623 8th Int. Brick Block Mason. Conf., Dublin, 1988: pp. 205–216.
- 624 [33] B.A. Güney, Development of Pozzolanic Lime Mortars for the Repair of Historic Masonry, Middle East Technical University,
625 2012.
- 626 [34] V. Nežerka, Z. Slížková, P. Tesárek, T. Plachý, D. Frankeová, V. Petráňová, Comprehensive study on mechanical properties
627 of lime-based pastes with additions of metakaolin and brick dust, *Cem. Concr. Res.* 64 (2014) 17–29.
628 doi:10.1016/j.cemconres.2014.06.006.
- 629 [35] CEN, EN 1015-11:2007 Methods of test for mortar for masonry - Part 11: Determination of flexural and compressive strength
630 of hardened mortar, (2007).
- 631 [36] C. Mazzotti, E. Sassoni, G. Pagliai, Determination of shear strength of historic masonries by moderately destructive testing of
632 masonry cores, *Constr. Build. Mater.* 54 (2014) 421–431. doi:10.1016/j.conbuildmat.2013.12.039.
- 633 [37] Z.P. Bažant, Concrete fracture models: testing and practice, *Eng. Fract. Mech.* 69 (2002) 165–205. doi:10.1016/S0013-
634 7944(01)00084-4.
- 635 [38] K. Chaimoon, M.M. Attard, Shear fracture in masonry joints, in: C.A. Brebbia (Ed.), 12th Int. Conf. Comput. Methods Exp.
636 Meas., WIT Press, Malta, 2005: pp. 205–215.
- 637 [39] N. Augenti, F. Parisi, Constitutive modelling of tuff masonry in direct shear, *Constr. Build. Mater.* 25 (2011) 1612–1620.
638 doi:10.1016/j.conbuildmat.2010.10.002.
- 639 [40] Z.P. Bažant, P.C. Prat, M.R. Tabbara, Antiplane Shear Fracture Tests (Mode III), *ACI Mater. J.* 87 (1990) 12–19.

- 640 [41] V. Nežerka, J. Zeman, J. Němeček, Micromechanics-based simulations of compressive and tensile testing on lime-based
641 mortars, *Mech. Mater.* 105 (2017) 49–60. doi:10.1016/j.mechmat.2016.11.011.
- 642 [42] EN 1015-1:1999, Methods of test for mortar for masonry - Part 1: Determination of particle size distribution (by sieve
643 analysis), (2007).
- 644 [43] EN 12390-1:2000, Testing hardened concrete - Part 1: Shape, dimensions and other requirements for specimens and moulds,
645 (2000).
- 646 [44] Circolare 02/02/2009 n. 617, Istruzioni per l'applicazione delle "Norme tecniche per le costruzioni" di cui al D.M. 14 gennaio
647 2008, (2009).
- 648 [45] L. Pelà, A. Benedetti, D. Marastoni, Interpretation of Experimental Tests on Small Specimens of Historical Mortars, in: J.
649 Jasieńko (Ed.), *Struct. Anal. Hist. Constr.*, DWE, Wrocław, Poland, 2012: pp. 716–723.
- 650 [46] UIC, Leaflet 778-3R: Recommendations for the inspection, assessment and maintainance of masonry arch bridges., (1995).
- 651 [47] C. Bilello, A. Brencich, C. Corradi, M. Di Paola, E. Sterpi, Experimental Tests and Theoretical Issues for the Identification of
652 Existing Brickwork, in: *10th North Am. Mason. Conf.*, St. Louis, Missouri, USA, 2007: pp. 964–974.
- 653 [48] A. Brencich, E. Sterpi, Compressive Strength of Solid Clay Brick Masonry: Calibration of Experimental Tests and
654 Theoretical Issues, in: P.B. Lourenço, P. Roca, C. Modena, S. Agrawal (Eds.), *Struct. Anal. Hist. Constr.*, New Delhi, India,
655 2006: pp. 757–766.
- 656

657 **Appendix A: Experimental data for the calibration of the TPT**

658 **A.1 Experimental campaign at University of Bologna**

659 The experimental program was based on the construction of a large set of cubic specimens of mortar. The
660 samples were prepared using different compositions in order to obtain a representative range of compressive
661 strengths. The manufacture was carried out in the Laboratory of Structural and Geotechnical Engineering
662 (LISG) of the University of Bologna, Italy.

663 Seven mixtures of mortar, properly designed in order simulate different materials behaviour, were used to build
664 the specimens. Each mixture was composed of different proportions of river sand ($0 \div 2$ mm grain size),
665 Portland Cement 32.5 R, Natural Hydraulic Lime NHL 3.5 and water. The proportions among the components
666 were carefully chosen following the common practice in masonry construction in order to obtain a statistically

667 significant range of compressive strengths. The mass proportions of components for each mortar mixture are
 668 reported in Table A.1.

669 Mixtures “A” were characterised by a water/binder mass ratio of about 0.5-0.6, according to the standard
 670 mortar composition. On the contrary, mixtures “B” had water/binder ratio around 1.0, reducing significantly the
 671 compressive strength of the specimens. For each mortar mixture, three specimens were casted using 150×150
 672 $\times 150 \text{ mm}^3$ PVC moulds. The samples were then stored for 28 days inside a climatic chamber (20°C and 98%
 673 RH). After the curing period, two holes were drilled in the centre of two opposite lateral surfaces of the
 674 samples. The faces selected for the penetrometric tests were those in contact with the moulds, granting the
 675 required planarity of the surfaces loaded during the compression test. The pilot hole was made by using a
 676 vertical driller with a hardened steel bit of 7 mm diameter. The pilot cavity was perfectly orthogonal to the
 677 investigated surface.

678 Table A.1 reports the readings of the TPT for each sample, expressed as normalised ultimate torque per unit
 679 length (m_v , in Nmm/mm) and the standard compressive strength (f_c , in MPa). Each value of m_v reported for each
 680 sample is the average of the two readings obtained from the two opposite lateral surfaces of the cube specimen,
 681 see Figure 8. More details about the experimental results of this testing program can be found in [21].

682

683 Table A.1 – Mortar mixture adopted in the experimental campaign and Torque Penetrometric Test results on cubic samples of mortar
 684 [21], normalised ultimate torque measured (m_v) and standard compressive strength (f_c).

Mix	NHL	Cem.	Sand	Water	Tot	m_v			f_c		
	[kg]	[kg]	[kg]	[kg]	[kg]	[Nmm/mm]			[MPa]		
						1	2	3	1	2	3
A1	5.0	-	15.0	3.0	23.0	350	433	333	1.31	1.43	1.33
A2	2.0	3.0	16.0	2.5	23.5	1067	1383	1250	8.55	8.68	8.52
A3	4.0	1.1	16.0	3.0	24.1	450	433	467	2.43	2.39	2.39
A4	3.5	2.5	15.0	2.7	23.7	1050	1250	1233	7.41	7.67	7.17
B2	3.4	-	18.0	3.0	24.4	167	217	-	0.45	0.46	-
B3	1.5	2.5	14.9	2.5	21.4	883	967	950	5.39	5.76	5.82

B4 | 1.0 1.5 18.0 2.5 | 23.0 | 367 517 500 | 1.82 1.78 1.81

685

686 A.2 Experimental campaign at DTI

687 The experimental program developed at DTI by Christiansen [20] used the X-Drill device. Several
 688 penetrometric tests were carried out on ten walls built in the laboratory and the results then compared with the
 689 standard tests on mortar according to the available standards for mortar [35]. The mortar specimens were
 690 obtained by using premixed mortars with different parts of lime, cement, aggregates and water content in the
 691 mixture. The premixed mortars were classified in two categories: dry mixes (the water was entirely added
 692 during the moulding phase) and wet mixes (mortar contained water and additional cement or water were
 693 added). The mortars were used to build 10 different walls with nominal mortar joint thickness of 12 mm. The
 694 tests were performed in the T-cross joints in order to reduce the risk of hitting the units. Table A.2 reports the
 695 compositions of the walls used for the calibration and the results of the standard compression test on the mortar
 696 specimens.

697 Moreover, Table A.2 presents, for every specimen of given compressive strength, the Christiansen's original
 698 data (normalised ultimate torque measured with X-Drill $m_{v,XDrill}$) and their adjusted values ($m_{v,TPT}$) evaluated
 699 according to the Equation 15.

700

701 Table A.2 - Mortar Mixtures used for the experimental campaign for the calibration of the X-Drill at DTI [20], name of the wall in
 702 which the mortar was used, type of mortar, dry/wet mixture and standard compressive strength of the specimens (f_c), normalised
 703 ultimate torque measured with X-Drill ($m_{v,XDrill}$) and adjusted values of the normalised ultimate torque to make possible the direct
 704 comparison with TPT readings ($m_{v,TPT}$).

Wall	Type	Dry/Wet	f_c [MPa]	$m_{v,X-drill}$ [Nmm/mm]	$m_{v,TPT}$ [Nmm/mm]
A	Design mortar	-	3.23	996	703
B	CL 40/60/850	WET	1.1	347	245
C	L 100/1200	WET	0.39	153	108

D	CL 50/50/700	DRY	4.99	1134	801
E	Design mortar	-	2.84	945	667
F	CL 40/60/850	WET	1.48	393	278
G	CL 40/60/850	WET	1.38	511	361
H	L 100/1200	WET	0.34	96	68
I	L 100/1200	WET	0.57	98	69
J	L 100/1200	DRY	0.4	175	124

705